Photopolymerization of Carbohydrate-Based Discotic Mesogens. Syntheses and Phase Properties of 1,2,3,4,6-Penta-*O*-(*trans*-3,4-dialkoxycinnamoyl)-(D)-glucopyranoses and Their Oligomers

Ravindranath Mukkamala,[†,‡] Charles L. Burns, Jr.,[†] Robert M. Catchings III,[§] and Richard G. Weiss*[,†]

Contribution from the Department of Chemistry, Georgetown University, Washington, DC 20057-1227, and Department of Physics and Astronomy, Howard University, Washington, DC 20059

Received May 17, 1996[⊗]

Abstract: The neat phase properties of the α and β anomers of 1,2,3,4,6-penta-*O*-(*trans*-3,4-dialkoxycinnamoyl)-(D)-glucopyranose (**n**α**GP** and **n**β**GP**; *n*, the number of carbon atoms in the alkyl chains, is 6−8, 10, and 14) have been investigated by optical microscopy, differential scanning calorimetry, and X-ray powder diffraction. Each of the **GP** forms an enantiotropic and thermotropic discotic columnar liquid−crystalline phase. Irradiation of the **14GP** in dilute solutions leads to two *intra*molecular [2 + 2] cycloaddition reactions between cinnamoyl double bonds. In the solid I (obtained by recrystallization from solvent and in which **14GP** molecules are paired in each columnar stack) and "isotropic" melt phases, only short (<10 monomer unit), probably branched oligomers form upon irradiation due to the continued preference for *intra*molecular cycloadditions and the ability of each monomer to interact with more than two neighbors. Irradiation of the solid II phase (obtained by cooling the liquid−crystalline phase) provides unbranched oligomers with <20 monomer units. However, more than 30 **14**α**GP** monomer units have been linked in unbranched chains upon irradiation of its liquid−crystalline phase. This is the greatest degree of columnar polymerization reported to date from a discotic mesophase. Qualitatively similar results are obtained upon irradiation of other **GP** in their various phases. *Oligomerization of **GP** liquid−crystalline and solid I phases is intracolumnar, and the columnar packing arrangement of the monomers is retained to ca. 100 °C above their clearing temperatures*; each **GP** produces nanoscale cylinders of one diameter but varying lengths. The oligomers unwind and do not retake their original form when they are dissolved and reprecipitated or heated to above their clearing temperatures and cooled. The nature of the oligomerization processes is discussed, especially with regard to *inter*-/*intra*molecular and *inter*-/*intra*columnar competitions for [2 + 2] cycloaddition reactions and the possibility of an anomeric effect on oligomer length.

Introduction

The synthesis of molecular objects with persistent shapes, nanoscale dimensions, and defined functions has become an important aspect of materials chemistry.[1,2] Polymers with cylindrical shapes, consisting of cofacially arranged disc-like monomer units, have been shown to possess superior mechanical properties, high temperature, and dimensional stability; they have also found applications in building photonic devices and one-dimensional charge carriers.[3,4] A logical route to cylindrically-shaped molecular objects is to preassemble disc-like monomers into columns and then to effect an *intracolumnar*−*intermolecular* polymerization (Scheme 1).[5] In this regard, columnar liquid-crystals offer obvious possibilities.

Recent studies have established that bulk polymerization of organized liquid−crystalline phases is an effective way to produce materials having interesting thermal, mechanical, optical, electrical, and magnetic properties.[6,7] Post-synthetic processing is not necessary because the long-range orientational order of monomers in their mesophases can be incorporated as a permanent part of the macroscopic network formed after polymerization. For example, some cholesteryl carbonates and esters in their cholesteric liquid−crystalline phases have been irradiated to obtain polymers with cholesteric optical properties

Scheme 1

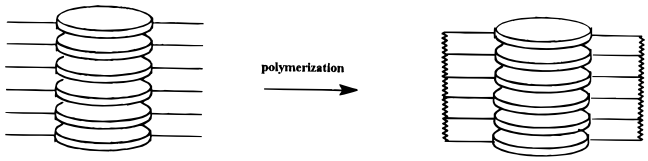

[†] Georgetown University.
[‡] Present address: Materials Science Division, Lawrence Berkeley National Laboratory, 1 Cyclotron Road, Berkeley, CA 94720.
[§] Howard University.
[⊗] Abstract published in *Advance ACS Abstracts,* October 1, 1996.

(1) Stupp, S. I.; Son, S.; Li, L. S.; Lin, H. C.; Keser, M. *J. Am. Chem. Soc.* **1995**, *117*, 5212.
(2) Lindsey, J. S. *New J. Chem.* **1991**, *15*, 153.
(3) Neher, D. *Adv. Mater.* **1995**, *7*, 691.
(4) (a) Adam, D.; Schumacher, P.; Simmerer, J.; Haussling, L.; Slemensmeyer, K.; Etzbach, K. H.; Ringsdorf, H.; Haarer, D. *Nature* **1994**, *371*, 141. (b) Disch, S.; Finkelmann, H.; Ringsdorf, H.; Schuhmacher, P. *Macromolecules* **1995**, *28*, 2424.
(5) (a) Mertesdorf, C.; Ringsdorf, H.; Stumpe, J. *Liq. Crystals* **1991**, *9*, 337. (b) Kurihara, S.; Ohta, H.; Nonaka, T. *Trans. Mat. Res. Soc. Jpn.* **1994**, *15A*, 357. (c) Baldvins, J. E. Ph.D. Thesis, Georgetown University, Washington, DC, 1995. (d) Meier, H.; Muller, K. *Angew. Chem., Int. Ed. Engl.* **1995**, *34*, 1437. (e) van Nostrum, C. F.; Picken, S. J.; Schouten, A.-J.; Nolte, R. J. M. *J. Am. Chem. Soc.* **1995**, *117*, 9957. (f) Clark, T. D.; Ghadiri, M. R. *J. Am. Chem. Soc.* **1995**, *117*, 12364.
(6) (a) Tsibouklis, J.; Feast, W. J. *Trends In Polym. Sci.* **1993**, *1*, 16. (b) Percec, V.; Jonsson, H.; Tomazos, D. In *Polymerization in Organized Media*; Paleos, C. M., Ed.; Gordon and Breach: Philadelphia, 1992; pp 1−104.
(7) (a) Shannon, P. J. *Mol. Cryst. Liq. Cryst.* **1984**, *110*, 135. (b) Shannon, P. J. *Macromolecules* **1984**, *17*, 1873. (c) Broer, D. J.; Gossink, R. G.; Hikmet, R. A. M. *Angew. Macromol. Chem.* **1990**, *183*, 45.

S0002-7863(96)01665-4 CCC: $12.00

that are retained even at very high temperatures.[7a,b] Similarly, polymerization of some smectic phases has produced uniaxially ordered polymeric networks with anisotropic optical and other physical properties.[7c] Recently, shape-persistent, slab-like two-dimensional polymers have been synthesized from monomeric smectic phases.[1]

Attempts to stabilize the columnar order of discotic mesogens by polymerization through intermolecular [2 + 2] cycloadditions of cinnamoyl double bonds have had limited success.[5a−c] For example, efforts to polymerize hexakis-*N*-(4-tetradecyloxycinnamoyl)hexacyclen (containing a flexible azacrown core) in its D_{ho} (hexagonal ordered) columnar discotic phase by *intracolumnar*−*intermolecular* photochemical [2 + 2] cycloadditions among the pendant cinnamoyl groups were unsuccessful due to a loss of liquid-crystallinity during irradiation caused by a parallel process, trans−cis isomerization of the double bonds.[5a] Similarly, photoinduced polymerization of hexakis-(4-octadecyloxycinnamoyloxy)triphenylene (containing a flat, rigid aromatic core) has been attempted:[5b] intermolecular coupling through [2 + 2] cycloadditions was inefficient in both the solid and D_{ho} phases, leading only to dimers and some oligomers of unspecified length; although irradiation of the N_D (nematic discotic) phase resulted in a higher degree of intermolecular reaction, liquid-crystallinity was lost.

Previously, we found that both the α and β anomers of a wide range of homologues of 1,2,3,4,6-penta-*O*-(*n*-alkanoyl)-(D)-glucopyranose (**GA**) aggregate into several types of columnar discotic phases.[8] They, like molecules based upon some inositols[9] and mono-, di-, and trisaccharides,[10] constitute a novel class of discotic liquid-crystals[11] with rather rigid, chiral cores. As an extension of that work, we sought to make disc-shaped glucopyranose molecules that are polymerizable in columnar stacks since glucopyranose, being more rigid than a hexacyclen[5a] and more flexible than a triphenylene,[5b] might allow pendant cinnamoyl groups to dimerize without loss of initial phase order. However, both the α and β anomers of the initially synthesized molecules, 1,2,3,4,6-penta-*O*-(*trans*-cinnamoyl)-(D)-glucopyranose (**GC**),[5c] were nonmesomorphic due to insufficient flexibility in the pendant groups.[12] In spite of this, irradiations of the **GC** in their neat melt, crystalline and glass phases reveal the decreasing importance of both trans−cis isomerization and *intra*molecular [2 + 2] cycloaddition reactions among cinnamoyl double bonds, and increasing efficiency of *inter*molecular [2 + 2] cycloadditions as phase order increases.[5c]

Here, we investigate the properties of ten α and β anomers of 1,2,3,4,6-penta-*O*-(*trans*-3,4-dialkoxycinnamoyl)-(D)-glucopyranoses (**nαGP** and **nβGP**, Scheme 2) that form discotic columnar liquid−crystalline phases. In addition to a determination of the neat **GP** phase structures, results from irradiations

Scheme 2

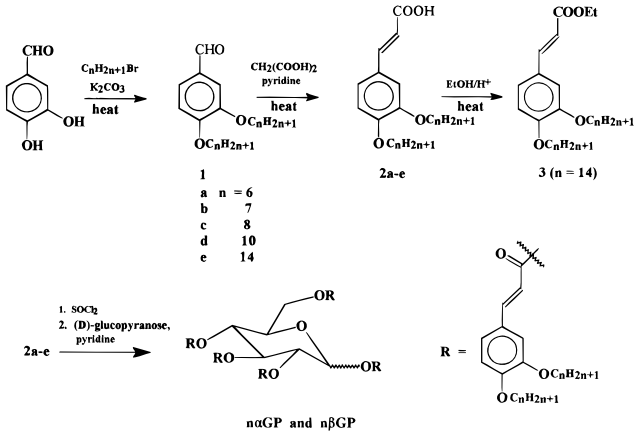

of a short and a long-chained homologue of **nαGP** and **nβGP** are reported.

Experimental Section

Materials and Methods. Benzene (Fisher, ACS grade) was dried over calcium chloride, azeotropically distilled, and stored over type 4A molecular sieves. Spectrograde benzene (Baker) was used as received. Pyridine (Fisher) was dried by distillation from calcium hydride and stored over type 4A molecular sieves. 3,4-Dihydroxybenzaldehyde (97%) from Lancaster and the 1-bromoalkanes (97−99%), malonic acid (99%), dipropyl amine (99%), thionyl chloride (99+%), oxalyl chloride (98%), and 4-dimethylaminopyridine (DMAP, 99%) from Aldrich were used as received. Anhydrous α-D-glucose (with 5% β anomer) and β-D-glucose (with 3% α anomer) from Sigma were dried under house vacuum at ca. 50 °C for 24 h before use.

Melting points (corrected) and photomicrographs were recorded on a Leitz 585 thermostatting stage between crossed polars with a Leitz Wetzlar (SM-LUX-POL) microscope and a mounted Pentax K1000 35 mm camera. Differential scanning calorimetry (DSC) was performed on a TA Instruments 2910 modulated differential scanning calorimeter, controlled by a Thermal Analyst 3100 using indium as standard for temperature and heat calibration. The rate of heating or cooling was 2°/min at lower temperatures and 3°/min in the higher temperature regions.

High-performance liquid chromatography (HPLC) was performed on a Waters Associates liquid chromatograph with a 254 nm absorbance detector and a 4.4 × 250 mm Alltech 5μ silica gel column using 5-15/95-85 ethyl acetate/hexane mixtures as eluents. Gel permeation chromatography was performed on either a Varian 5500 liquid chromatograph with a Varian RI-4 refractive index detector or a Hewlett Packard series 1050 liquid chromatograph with a Wyatt/Optilab 903 refractive index detector, equipped with two polystyrene columns (6.2 × 250 mm Zorbax PSM Bimodel-S or 6.2 × 250 mm Altex μ Sphereogel) connected in series and calibrated with at least four different polystyrene standards (Polysciences, Inc.). Tetrahydrofuran (THF, HPLC grade) was the eluent at a flow rate of 1.0 mL/min.

UV/vis absorption spectra were recorded on a Perkin-Elmer Lambda 6 UV/vis spectrophotometer and were analyzed using Perkin-Elmer PECSS software. Circular dichroism (CD) spectra were recorded on a JASCO J-710 spectropolarimeter using a Hellma jacketed quartz cell of 0.1 mm path length. Proton NMR spectra were recorded on a Bruker 270 MHz nuclear magnetic resonance spectrometer with a Tecmag operating system. IR spectra were recorded on a MIDAC FT-IR spectrometer as KBr pellets or chloroform solutions. Elemental analyses were performed by Desert Analytics, Tucson, AZ.

Powder X-ray diffraction patterns were collected on samples in copper discs with flat indentations using a Scintag 2000 X-ray powder diffractometer equipped with a liquid N_2 cooled solid state Ge detector and Cu Kα radiation (1.5406 Å). The copper holders were heated on a hot plate until the samples melted, placed quickly on the heated (to ca. 50 °C) sample holder of the diffractometer, and then allowed to equilibrate for about 15 min. The final temperatures were usually between 52−54 °C. Data were collected between 0.5° and 35° in 2θ at a scan rate of 1−3°/min with an increment of 0.03°.

(8) Morris, N. L.; Zimmerman, R. G.; Jameson, G. B.; Dalziel, A. W.; Reuss, P. M.; Weiss, R. G. *J. Am. Chem. Soc.* **1987**, *110*, 2177.

(9) (a) Jeffrey, G. A.; Wingert, L. M. *Liq. Crystals* **1992**, *12*, 179. (b) Kohne, B.; Praefcke, K. *Angew. Chem., Int. Ed. Engl.* **1984**, *23*, 82. (c) Praefcke, K.; Marquardt, P.; Kohne, B.; Stephan, W.; Levelut, A.-M.; Wachtel, E. *Mol. Cryst. Liq. Cryst.* **1991**, *203*, 149. (d) Praefcke, K.; Blunk, D.; Hempel, J. *Mol. Cryst. Liq. Cryst.* **1994**, *243*, 323.

(10) (a) Vill, V.; Thiem, J. *Liq. Crystals* **1991**, *9*, 451. (b) Takada, A.; Itoh, T.; Fukuda, T.; Miyamoto, T. *Bull. Inst. Chem. Res., Kyoto Univ.* **1991**, *69*, 77. (c) Sugiura, M.; Minoda, M.; Fukuda, T.; Miyamoto, T.; Watanabe, J. *Liq. Crystals* **1992**, *12*, 603. (d) Takada, A.; Ide, N.; Fukuda, T.; Miyamoto, T.; Yamagata, K.; Watanabe, J. *Liq. Crystals* **1995**, *19*, 441. (e) Zimmermann, R. G.; Jameson, G. B.; Weiss, R. G.; Demailly, G. *Mol. Cryst. Liq. Cryst. (Letters)* **1985**, *1*, 183.

(11) (a) Chandrasekhar, S.; Sadashiva, B. K.; Suresh, K. A. *Pramana* **1977**, *9*, 471. (b) Hinov, H. P. *Mol. Cryst. Liq. Cryst.* **1986**, *136*, 221. (c) Chandrasekhar, S.; Ranganath, G. S. *Rep. Prog. Physics* **1990**, *53*, 57. (d) Chandrasekhar, S. *Liquid Crystals*; Cambridge University Press: New York, 1992. (e) Weiss, R. In *Polymer Liquid Crystals. Thermophysical and Mechanical Properties*; Brostow, W., Ed.; Chapman and Hall: London, Vol. 3, accepted.

(12) Collings, P. J. *Liquid Crystals*, Princeton University Press: NJ, 1990.

Irradiations employed a 220 W Black-Ray long-wavelength UV lamp (320−360 nm). Samples of known mass between Pyrex cover slips, separated in some cases by teflon rings of known thickness, were kept on a Thomas thermostatting stage (about 15 cm from the lamp) mounted on a Bausch & Lomb microscope. After specific periods of irradiation, the Pyrex cover slips were carefully broken into small pieces and sonicated for ca. 20 min in chloroform to dissolve the samples and to make solutions of known concentrations. Decreases in optical densities of these solutions at 333 nm, normalized to constant weight, were used to approximate the photoconversions.

Molecular mechanics (force field) calculations (MM^+ method) were conducted with a program available as part of the Hyperchem package[13] using the Polak-Ribiere (conjugate gradient) algorithm and an RMS gradient termination condition of 0.1 Kcal/Å-mol.

Syntheses. A general outline of the synthetic procedures for the **GP** is shown in Scheme 2.

3,4-Dialkyloxybenzaldehydes (1a−e). A mixture of 3,4-dihydroxybenzaldehyde (6.9 g, 50 mmol), 1-bromoalkane (140 mmol), and anhydrous K_2CO_3 (34.5 g, 250 mmol) in 200 mL of 2-butanone was heated under reflux with stirring for 24 h in a dry atm. Most of the solvent was removed on a rotary evaporator, and ca. 200 mL water and ca. 250 mL chloroform were added. The organic layer was separated from the aqueous layer, washed with more water (3 × 150 mL), and dried (anhydrous Na_2SO_4). Evaporation of the solvent afforded the crude product. The hexyloxy homologue (**1a**) was used without further purification, **1b**−**d** were purified by column chromatography (silica gel, hexane followed by 1/1 hexane/chloroform), and **1e** was recrystallized from acetone. Product yields were typically 70−80%: **1b**, mp 47−49 °C (lit.[14] mp 48 °C); **1c**, mp 52−54 °C (lit.[14] mp 55 °C); **1d**, mp 62 °C (lit.[14] mp 65 °C); **1e**, mp 76−78 °C (lit.[14] mp 78 °C). IR and ^{1}H NMR spectra are consistent with the assigned structures.

3,4-Dialkoxycinnamic acids (2) were prepared by the procedure described for **2a**. A mixture of 3,4-dihexyloxybenzaldehyde (crude material from the previous reaction, ca. 40 mmol), malonic acid (10.4 g, 100 mmol), 120 mL of pyridine, and 35 mL of dipropyl amine was heated with stirring at ca. 110 °C for 1.5 h in a dry atm. The reaction mixture was cooled to ca. 40 °C and then poured into a mixture of 300 mL of concentrated HCl and ca. 300 g of ice. The crude product was collected by filtration, washed with ca. 600 mL water, suction-dried, and recrystallized (chloroform/hexane and ethanol) to yield 4.1 g (23% from 3,4-dihydroxybenzaldehyde) of light brown solid, mp 124−127 °C. IR (KBr) 3300−2340 (broad, acid O−H), 1662 (C═O), 1595 cm^{-1} (aromatic); ^{1}H NMR (270 MHz, $CDCl_3$/TMS) δ 7.7 (d, J = 15.8 Hz, 1H, olefinic), 7.1 (m, 2H, aromatic), 6.9 (d, J = 7.9 Hz, 1H, aromatic), 6.3 (d, J = 16.0 Hz, 1H, olefinic), 4.0 (m, 4H, -*O*-CH_2-), 1.9−0.8 (m, 22H, aliphatic).

3,4-Diheptyloxycinnamic acid (2b) was obtained in 35% yield as a light brown solid (recrystallized from ethanol), mp 124.6−128.8 °C. IR (KBr) 3184−2500 (broad, acid O−H), 1664 (C═O), 1622 (olefinic C═C) 1595 (aromatic) cm^{-1}; ^{1}H NMR (270 MHz, $CDCl_3$/TMS) δ 7.7 (d, J = 15.8 Hz, 1H, olefinic), 7.1 (m, 2H, aromatic), 6.85 (d, J = 8.3 Hz, 1H, aromatic), 6.3 (d, J = 15.8 Hz, 1H, olefinic), 4.0 (m, 4H, -*O*-CH_2-), 1.9−0.8 (m, 26H, aliphatic).

3,4-Dioctyloxycinnamic acid (2c) was obtained in 38% yield as a light brown solid (recrystallized from acetic acid), mp 125.1−129.2 °C. IR (KBr) 3280−2380 (broad, acid O−H), 1664 (C═O), 1662 (olefinic C═C), 1595 (aromatic) cm^{-1}; ^{1}H NMR (270 MHz, $CDCl_3$/TMS) δ 7.7 (d, J = 15.8 Hz, 1H, olefinic), 7.1 (m, 2H, aromatic), 6.85 (d, J = 8.3 Hz, 1H, aromatic), 6.3 (d, J = 15.8 Hz, 1H, olefinic), 4.0 (m, 4H, -*O*-CH_2-), 1.9−0.8 (m, 30H, aliphatic).

3,4-Didecyloxycinnamic acid (2d) was obtained in 42% yield as white solid (recrystallized from acetic acid), mp 123.8−128.3 °C. IR (KBr) 3200−2400 (broad, acid O−H), 1664 (C═O), 1622 (olefinic C═C), 1595 (aromatic) cm^{-1}; ^{1}H NMR (270 MHz, $CDCl_3$/TMS) δ 7.7 (d, J = 15.8 Hz, 1H, olefinic), 7.1 (m, 2H, aromatic), 6.85 (d, J = 8.1 Hz, 1H, aromatic), 6.3 (d, J = 15.8 Hz, 1H, olefinic), 4.0 (m, 4H, -*O*-CH_2-), 1.9−0.8 (m, 38H, aliphatic).

3,4-Ditetradecyloxycinnamic acid (2e) was eluted by column chromatography (silica gel, 7/3 chloroform/hexane) and recrystallized from ethanol/chloroform to give a 36% yield of a white solid, mp 124.6−127.8 °C. IR (KBr) 3300−2400 (broad, acid O−H), 1662 (C═O), 1622 (olefinic C═C), 1595 (aromatic) cm^{-1}; ^{1}H NMR (270 MHz, $CDCl_3$/TMS) δ 7.7 (d, J = 16.0 Hz, 1H, olefinic), 7.1 (m, 2H, aromatic), 6.85 (d, J = 8.0 Hz, 1H, aromatic), 6.3 (d, J = 15.8 Hz, 1H, olefinic), 4.0 (m, 4H, -*O*-CH_2-), 1.9−0.8 (m, 54H, aliphatic).

1,2,3,4,6-Pentakis-*O*-(*trans*-3,4-dialkyloxycinnamoyl)-(D)-glucopyranoses (nαGP and nβGP). All manipulations were performed in dim light to minimize photodecomposition. 3,4-Dialkyloxycinnamic acid (3.5−4.0 mmol) and an excess of thionyl chloride (5 mL) in 5 mL of dry benzene were stirred at ca. 60 °C for 1 h in a dry atm. Excess thionyl chloride and benzene were distilled at atmospheric pressure. Additional dry benzene (2 × 10 mL) was added, distilled as before, and an aspirator vacuum (protected by anhydrous $CaSO_4$ and sodium hydroxide) was applied to the residue for 45 min at ca. 60 °C to remove traces of thionyl chloride. The crude acid chloride was dissolved in 10 mL of dry pyridine, and ca. 0.5 mmol of α- or β-D-glucopyranose and ca. 20 mg of DMAP were added to the solution. The reaction mixture was stirred in the dark and in a dry atmosphere for 24 h at ca. 60 °C, poured into a mixture of 30 g of ice and 50 mL concentrated HCl, and extracted with ca. 300 mL of chloroform. The organic layer was washed sequentially with water, aqueous $NaHCO_3$, and water. After being dried (anhydrous Na_2SO_4), solvent was removed (rotary evaporator) to afford a dark yellow-brown solid which was eluted by column chromatography (silica gel, 60−200 mesh). The resulting light brown-yellow solids were recrystallized to obtain white or light yellow powders. Details of specific solvent mixtures used for column chromatography and recrystallization of different homologues are available as supporting information.

1,2,3,4,6-Pentakis-*O*-(*trans*-3,4-dihexyloxycinnamoyl)-β(D)-glucopyranose (6βGP): 45% yield of a pale yellow, amorphous solid (99% pure by HPLC), mp ca. 72 °C (solid to mesophase) and 85.2−86.1 °C (mesophase to isotropic). IR (KBr) 2930, 2870, 1718 (ester C═O), 1633 (C═C) cm^{-1}; ^{1}H NMR (270 MHz, $CDCl_3$/TMS) δ 7.7−7.5 (m, 5H, olefinic), 7.1−6.75 (two m, 15H, aromatic), 6.4−6.0 (m, 6H, olefinic and -COO-CH-), 5.7−5.4 (m, 3H, -COO-CH-), 4.4 (broad m, 2H, -COO-CH-), 4.2−3.9 (m, 21H, -COO-CH- and -*O*-CH_2-), 1.9−0.8 (m, 110H, aliphatic). Anal. Calcd for $C_{111}H_{162}O_{21}$: C, 72.79; H, 8.85. Found: C, 73.03; H, 9.02.

1,2,3,4,6-Pentakis-*O*-(*trans*-3,4-dihexyloxycinnamoyl)-α(D)-glucopyranose (6αGP): 9% yield of a pale yellow solid (>99% pure by HPLC), mp ca. 50 °C (solid to mesophase) and 60.4−62.0 °C (mesophase to isotropic). IR (KBr) 2932, 2872, 1718 (ester C═O), 1631 (C═C) cm^{-1}; ^{1}H NMR (270 MHz, $CDCl_3$/TMS) δ 7.8−7.5 (m, 5H, olefinic), 7.2−5.9 (several m, 22H, aromatic, olefinic and -COO-CH-), 5.6−5.4 (m, 2H, -COO-CH-), 4.4 (broad m, 3H, -COO-CH-), 4.1−3.9 (m, 20H, -*O*-CH_2-) and 1.9−0.8 (m, 110H, aliphatic). Anal. Calcd for $C_{111}H_{162}O_{21}$: C, 72.79; H, 8.85. Found: C, 72.77; H, 8.66.

1,2,3,4,6-Pentakis-*O*-(*trans*-3,4-diheptyloxycinnamoyl)-β(D)-glucopyranose (7βGP): 28% yield of a pale yellow solid (>97% pure by HPLC), mp ca. 78 °C (solid to mesophase) and 104.8−105.6 °C (mesophase to isotropic). IR (KBr) 2930, 2856, 1718 (ester C═O), 1633 (C═C) cm^{-1}; ^{1}H NMR (270 MHz, CDCl3) δ 7.7−7.5 (m, 5H, olefinic), 7.1−6.7 (two m, 15H, aromatic), 6.4−6.0 (m, 6H, olefinic and -COO-CH-), 5.7−5.4 (m, 3H, -COO-CH-), 4.4 (broad m, 2H, -COO-CH-), 4.2−3.9 (m, 21H, -COO-CH- and -*O*-CH_2-), 1.9−0.8 (m, 130H, aliphatic). Anal. Calcd for $C_{121}H_{182}O_{21}$: C, 73.71; H, 9.24. Found: C, 73.81; H, 9.25.

1,2,3,4,6-Pentakis-*O*-(*trans*-3,4-diheptyloxycinnamoyl)-α(D)-glucopyranose (7αGP): 17% yield as a light yellow solid (>99% pure by HPLC), mp ca. 50 °C (solid to mesophase) and 80.1−81.2 °C (mesophase to isotropic). IR (KBr) 2926, 2856, 1718 (ester C═O), 1631 (C═C) cm^{-1}; ^{1}H NMR (270 MHz, $CDCl_3$/TMS) δ 7.8−7.5 (m, 5H, olefinic), 7.2−5.9 (several m, 22H, aromatic, olefinic and -COO-CH-), 5.6−5.4 (m, 2H, -COO-CH-), 4.4 (broad m, 3H, -COO-CH-), 4.1−3.9 (m, 20H, -*O*-CH_2-) and 1.9−0.8 (m, 130H, aliphatic). Anal. Calcd for $C_{121}H_{182}O_{21}$: C, 73.71; H, 9.24. Found: C, 73.91; H, 9.28.

1,2,3,4,6-Pentakis-*O*-(*trans*-3,4-dioctyloxycinnamoyl)-β(D)-glucopyranose (8βGP). Following the general procedure, a mixture of the cinnamoyl chloride, β-D-glucopyranose, pyridine, and benzene was stirred at room temperature for 96 h under a dry atmosphere. Ethanol (200 mL) was added, and the solid that formed was collected by filtration and recrystallized from dichloromethane/ethanol to afford 22%

(13) By Hyper Cube Inc.

(14) Nguyen, H. T.; Destrade, C.; Malthete, J. *Liq. Crystals* **1990**, *8*, 797.

yield of a white solid (99% pure by HPLC), mp ca. 60 °C (solid to mesophase) and 110.6−111.7 °C (mesophase to isotropic). IR (thin film) 2926, 2854, 1717 (ester C═O), 1634 (C═C) cm^{-1}; ^1H NMR (270 MHz, $CDCl_3$/TMS) δ 7.65−7.4 (m, 5H, olefinic), 7.0−6.65 (two m, 15H, aromatic), 6.3−5.95 (m, 6H, olefinic and -COO-CH-), 5.65−5.35 (m, 3H, -COO-CH-), 4.35 (broad m, 2H, -COO-CH-), 4.1−3.8 (m, 21H, -COO-CH- and -*O*-CH_2-), 1.9−0.8 (m, 150H, aliphatic). Anal. Calcd for $C_{131}H_{202}O_{21}$: C, 74.50; H, 9.57. Found: C, 74.73; H, 9.69.

1,2,3,4,6-Pentakis-*O*-(*trans*-3,4-dioctyloxycinnamoyl)-α(D)-glucopyranose (8αGP): 10% yield of a pale yellow solid (>98% pure by HPLC), mp ca. 60 °C (solid to mesophase) and 90.1−91.2 °C (mesophase to isotropic). IR (thin film) 2926, 2855, 1719 (ester C═O), 1631 (C═C) cm^{-1}; ^1H NMR (270 MHz, $CDCl_3$/TMS) δ 7.8−7.5 (m, 5H, olefinic), 7.2−5.9 (several m, 22H, aromatic, olefinic and -COO-CH-), 5.6−5.4 (m, 2H, -COO-CH-), 4.4 (broad m, 3H, -COO-CH-), 4.1−3.9 (m, 20H, -*O*-CH_2-) and 1.9−0.8 (m, 130H, aliphatic). Anal. Calcd for $C_{131}H_{202}O_{21}$: C, 74.50; H, 9.57. Found: C, 74.26; H, 9.53.

1,2,3,4,6-Pentakis-*O*-(*trans*-3,4-didecyloxycinnamoyl)-β(D)-glucopyranose (10βGP): 17% yield of a pale yellow solid (>98% pure by HPLC), mp ca. 50 °C (solid to mesophase) and 121.9−123.1 °C (mesophase to isotropic). IR (thin film) 2923, 2853, 1717 (ester C═O), 1633 (C═C) cm^{-1}; ^1H NMR (270 MHz, $CDCl_3$/TMS) δ 7.7−7.5 (m, 5H, olefinic), 7.1−6.7 (two m, 15H, aromatic), 6.35−6.0 (m, 6H, olefinic and -COO-CH-), 5.7−5.4 (m, 3H, -COO-CH-), 4.4−3.8 (three m, 23H, -COO-CH- and -*O*-CH_2-), 1.9−0.8 (m, 190H, aliphatic). Anal. Calcd for $C_{151}H_{242}O_{21}$: C, 75.82; H, 10.13. Found: C, 75.76; H, 10.27.

1,2,3,4,6-Pentakis-*O*-(*trans*-3,4-didecyloxycinnamoyl)-α(D)-glucopyranose (10αGP): 8% yield of a pale yellow solid (98% pure by HPLC), mp ca. 50 °C (solid to mesophase) and 102.7−103.9 °C (mesophase to isotropic). IR (KBr) 2924, 2854, 1718 (ester C═O), 1633 (C═C) cm^{-1}; ^1H NMR (270 MHz, $CDCl_3$/TMS) δ 7.8−7.5 (m, 5H, olefinic), 7.2−5.9 (several m, 22H, aromatic, olefinic and -COO-CH-), 5.6−5.4 (m, 2H, -COO-CH-), 4.4 (broad m, 3H, -COO-CH-), 4.1−3.9 (m, 20H, -*O*-CH_2-) and 1.9−0.8 (m, 190H, aliphatic). Anal. Calcd for $C_{151}H_{242}O_{21}$: C, 75.82; H, 10.13. Found: C, 75.81; H, 10.29.

1,2,3,4,6-Pentakis-*O*-(*trans*-3,4-ditetradecyloxycinnamoyl)-β(D)-glucopyranose (14βGP): 37% yield of a white solid (99% pure by HPLC), mp ca. 75 °C (solid to mesophase) and 117.4−118.5 °C (mesophase to isotropic). IR (KBr) 2924, 2854, 1718 (ester C═O), 1633 (C═C) cm^{-1}; ^1H NMR (270 MHz, $CDCl_3$/TMS) δ 7.7−7.5 (m, 5H, olefinic), 7.1−6.7 (two m, 15H, aromatic), 6.4−6.0 (m, 6H, olefinic and -COO-CH-), 5.7−5.4 (m, 3H, -COO-CH-), 4.4−3.9 (three m, 23H, -COO-CH- and -*O*-CH_2-), 1.9−0.8 (m, 270H, aliphatic). Anal. Calcd for $C_{191}H_{322}O_{21}$: C, 77.69; H, 10.92. Found: C, 77.56; H, 10.95.

1,2,3,4,6-Pentakis-*O*-(*trans*-3,4-ditetradecyloxycinnamoyl)-α(D)-glucopyranose (14αGP): 17% yield of a white amorphous solid (>97% pure by HPLC), mp ca. 70 °C (solid to mesophase) and 104.6−106.5 °C (mesophase to isotropic). IR (KBr) 2920, 2851, 1718 (ester C═O), 1633 (C═C) cm^{-1}; ^1H NMR (270 MHz, $CDCl_3$/TMS) δ 7.8−7.5 (m, 5H, olefinic), 7.2−5.9 (several m, 22H, aromatic, olefinic and -COO-CH-), 5.6−5.4 (m, 2H, -COO-CH-), 4.5−3.9 (two broad m, 23H, -COO-CH- and -*O*-CH_2-) and 1.9−0.8 (m, 270H, aliphatic). Anal. Calcd for $C_{191}H_{322}O_{21}$: C, 77.69; H, 10.92. Found: C, 77.72; H, 10.69.

Ethyl *trans*-3,4-Ditetradecyloxycinnamate (3). A mixture of 3,4-ditetradecyloxycinnamic acid (0.55 g, 0.96 mmol), 40 mL of absolute ethanol, 15 mL of dry benzene, and 1 mL of concentrated sulfuric acid was heated under reflux with stirring for 20 h in the dark. Chloroform (150 mL) was added to the cooled reaction mixture, and the organic layer was washed sequentially with water, aqueous $NaHCO_3$, and water. After being dried (anhydrous Na_2SO_4), solvent was removed (rotary evaporator) to afford a light yellow solid which was eluted by column chromatography (silica gel, 60−200 mesh, 1/99 ethyl acetate/hexane) to obtain 0.2 g (35%) of a white solid (>99% pure by HPLC), mp 66.5−67.6 °C. IR (thin film) 2915, 2847, 1706 (C═O), 1631 (C═C) cm^{-1}; ^1H NMR (270 MHz, $CDCl_3$/TMS) δ 7.6 (d, J = 15.8 Hz, 1H, olefinic), 7.1−7.0 (m, 2H, aromatic), 6.85 (d, J = 8.8 Hz, 1H, aromatic), 6.3 (d, J = 15.8 Hz, 1H, olefinic), 4.25 (q, J = 7.0 Hz, 2H, -$COOCH_2$-), 4.0 (m, 4H, -*O*-CH_2-), 1.9−0.8 (m, 57H, aliphatic).

Results and Discussion

In an initial attempt to induce liquid-crystallinity in discotic molecules like **GC**, alkoxy chains of various lengths (-OC_nH_{2n+1}, n = 5−14) were attached at the *para* position of the cinnamoyl rings. However, neither the neat homologues nor their mixtures in various proportions[15] were liquid−crystalline.[16] Since one chain per cinnamoyl group is probably insufficient to fill the interstices near the glucopyranose cores, alkoxy chains were then placed at both the *meta* and *para* positions. The resultant disk-shaped molecules, **nαGP** and **nβGP**, form the desired discotic columnar liquid−crystalline phases.[17] Optical microscopic (OM) and differential scanning calorimetric (DSC) analyses demonstrate that the liquid−crystalline phases of all of the **nαGP** and **nβGP** are enantiotropic. Designations of the mesophases as discotic columnar liquid-crystals and of the molecular packing arrangements in solid phases are based upon powder X-ray diffraction (XRD) and optical microscopy data at appropriate temperatures.

To predict the shapes and structures of oligomeric products obtained from irradiation of the neat phases of the **GP**, their molecular packing and its topological consequences on intermolecular reactivity must be known. Prior studies employing [2 + 2] cycloaddition reactions of cinnamate double bonds have demonstrated clearly the need for proximity and orientational specificity if reaction selectivity is to be attained.[18]

The design of **GP** molecules places the reactive double bonds near the core and in conformations that make **GP** appear disk-shaped; the alkyl chains lie along the molecular periphery. In this way, *inter*columnar [2 + 2] cycloaddition reactions between cinnamate double bonds are blocked when the molecules are stacked in columns. Such packing does *not* preclude *intra*molecular [2 + 2] reactions which compete with the *intra*columnar−*inter*molecular reactions leading to oligomerization. Additionally, there are features of the **GP** that enhance the possibility of intermolecular linkages and oligomerizations in their columns: (1) the reactive cinnamoyl groups are projected *both* above and below the rough plane defined by the glucopyranose ring and (2) the **GP** contain an odd number of reactive groups. Thus, even if two pairs of cinnamate double bonds react intramolecularly, the fifth cannot and will be available for intermolecular reactions exclusively. However, at least *two* intermolecular reactions per **GP**, involving two different neighbors is the minimum requirement for columnar polymerization along a column. The dissymmetry of the projections of the five cinnamate groups of each **GP** has other desirable consequences with respect to columnar oligomerization. In more symmetrical and (especially) planar discotic molecules, the initial [2 + 2] cycloaddition favors subsequent reactions of other double bonds within the same molecular pair.[5d] As such, oligomerization is intrinsically disfavored.

Structures of GP Phases. Optical Microscopy. Upon being heated, samples sandwiched between cover slips underwent solid-to-liquid crystal transitions (K-D) that were difficult to measure precisely over ranges less than 1−2°, but liquid crystal-to-isotropic transitions (D-I) were more easily detected. The patterns became increasingly birefringent and deformable at higher temperatures. Optical textures between crossed polars

(15) It is possible, in some cases, to introduce mesomorphism in homologous mixtures of non-mesomorphic materials. See: Sheikh-Ali, B. M.; Weiss, R. G. *Liq. Crystals* **1994**, *17*, 605.

(16) Burns, C. L., Jr.; Weiss, R. G. Unpublished results.

(17) Mukkamala, R.; Burns, C. L., Jr.; Weiss, R. G. 29th ACS Middle Atlantic Regional Meeting, May 1995, Washington, DC, Abstract no. 255.

(18) For details on cinnamate photochemistry in anisotropic phases, see: (a) Schmidt, G. M. J., et al. *Solid State Photochemistry*; Ginsburg, D., Ed.; Verlag-Chemie: Weinheim, 1976. (b) Venkatesan, K.; Ramamurthy, V. In *Photochemistry in Organized and Constrained Media*; Ramamurthy, V., Ed.; VCH: Weinheim, 1991; pp 133−184. (c) Weiss, R. G. In *Photochemistry in Organized and Constrained Media*; Ramamurthy, V., Ed.; VCH: Weinheim, 1991; pp 603−690. (d) Enkelman, V.; Wegner, G.; Novak, K.; Wagener, K. B. *J. Am. Chem. Soc.* **1993**, *115*, 203. (e) Greiving, H.; Hopf, H.; Jones, P. G.; Bubenitschek, P.; Desvergne, J. P.; Bouas-Laurent, H. *J. Chem. Soc., Chem. Commun*. **1994**, 1075.

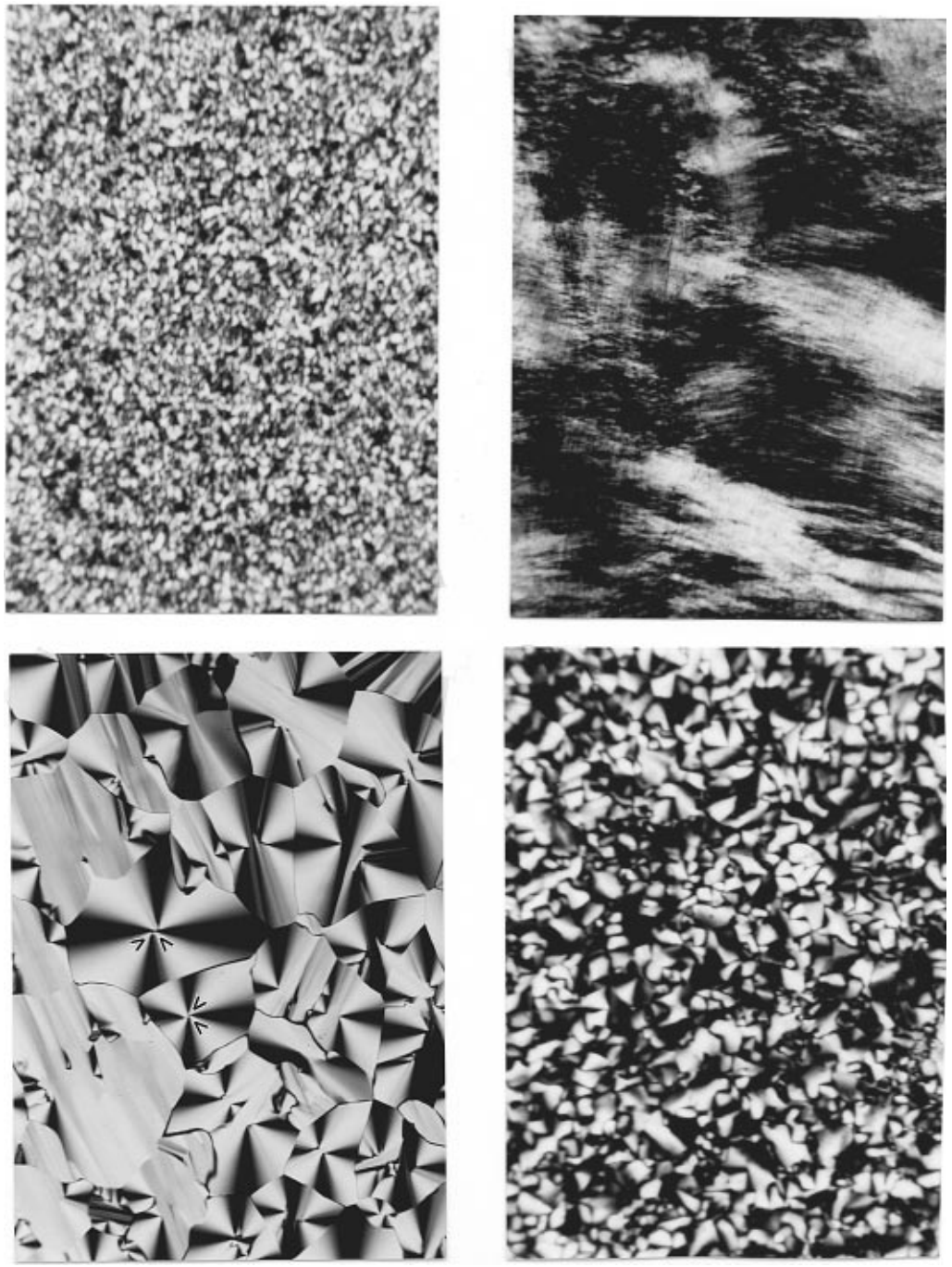

Figure 1. Optical mesophase textures of (a, top left) **7αGP** at 63 °C (× 560), (b, top right) **8βGP** at 81 °C, after shearing (× 340), (c, bottom left) **14βGP** at 102 °C (× 340) upon cooling the isotropic phase, and (d, bottom right) **14αGP** at 89 °C (× 700) upon cooling from the isotropic phase.

of the mesophases of **6αGP** and **7αGP** from heating or cooling were very similar (Figure 1a) and did not change with gentle pressing/shearing. For the other α homologues and the β anomers, gentle pressing/shearing motions resulted in textures from aligned mesophases (Figure 1b) that were distinctly different from those obtained upon slow cooling of the undisturbed isotropic phases (Figures 1c,d); textures similar to those in Figure 1b−d have been observed for the hexagonal discotic (D_h) mesophases of cellobiose octa(*n*-alkanoates).[10b]

The liquid crystal-to-solid transitions (D-K) of cooled samples were difficult to detect optically as well. The mesophases became increasingly viscous and gradually lost most of their birefringence while the optical textures were frozen in a glassy state. When reheated, the samples regained their highly birefringent appearance and fluidity.

The enantiomers of a triphenylene-based columnar discotic liquid crystal with optically active side chains have been observed to give nonsuperimposable fan-shaped textures (similar to Figure 1c) with only one type of fan pairs with opposite points.[19] Although the **GP** are chiral and optically pure, well-defined focal-conic (fan-shaped) textures with "off-centered meeting points" are observed only for **7**-, **8**-, **10**-, and **14βGP**. Even in these cases, the direction of the off-centered points appears to be somewhat random (points indicated by arrows in Figure 1c).

Differential Scanning Calorimetry. Mesophases of many **GP** have a tendency to supercool significantly before crystallizing. For that reason, samples were incubated at room temperature for 24 h and 2−3 weeks before recording the second and third heating−cooling cycles, respectively. Except for **6αGP** and **7αGP**, the D-K transition in cooling thermograms was not observed above room temperature. However, the I-D

(19) Malthete, J.; Jacques, J.; Tinh, N. H.; Destrade, C. *Nature* **1982**, *298*, 46.

Table 1. Solid-Mesophase (K-D) and Mesophase-Isotropic (D-I) Transition Temperatures (T, °C, Endotherm Peak Maxima) and Enthalpies (ΔH, Jg^{-1}) and Entropies (ΔS, $Jg^{-1}\,K^{-1}$) of **GP** from First and Second DSC Heating Scans

compd		first heating			second heating[a]		
		T	ΔH	$\Delta S \times 10^3$	T	ΔH	$\Delta S \times 10^3$
6α**GP**	K-D	58.1	4.15		57.8	6.04	
	D-I	62.4	2.93	8.7	62.0	3.27	9.8
7α**GP**	K-D	57.4	4.99		58.7	7.20	
	D-I	81.0	5.24	14.8	81.4	5.21	14.7
8α**GP**	K-D	48.7	6.12		47.2	4.94	
	D-I	90.8	5.66	15.6	91.1	5.86	16.0
10α**GP**	K-D	45.2	4.51		42.6	6.10	
	D-I	102.9	5.56	14.8	102.8	5.79	15.4
14α**GP**	K-D	54.1	42.0[b]		41.4	22.68	
	D-I	106.6	6.22	16.5	106.4	5.86	15.4
6β**GP**	K-D	53.4	2.54			*c*	
	D-I	84.2	1.93	5.4	84.7	1.88	5.3
7β**GP**	K-D	56.1	3.25			*c*	
	D-I	105.5	3.05	8.0	105.5	2.95	7.7
8β**GP**	K-D	64.3	14.15			*c*	
	D-I	113.6	3.20	8.3	113.8	2.99	7.7
10β**GP**	K-D		*c,d*			*c*	
	D-I	120.8	4.29	10.9	120.6	4.09	10.3
14β**GP**	K-D	55.4	46.27[b]		41.9	38.75	
	D-I	119.9	4.34	11.0	120.0	4.18	10.6

[a] Twenty-four h at ca. 25 °C after first heating/cooling scan. [b] Combined heat of multiple transitions. [c] Transition not observed. [d] Appearance is a soft solid at room temperature.

transitions showed no significant supercooling, as expected for enantiotropic phases.

For reasons that remain to be determined, the β anomers have a greater tendency to form glass phases than the α anomers. No K-D transition was detected in the second or third heating scans of **7**β**GP**, **8**β**GP**, and **10**β**GP**, and no K-D transition was observed for **10**β**GP** even in the first heating scan, although it appears to be a soft solid at room temperature (Table 1 and supporting information).

From Table 1, the temperatures of the K-D transitions (T_{K-D}) from the second heating scans change very little with increasing chain length in both the α- and β-anomeric series, while the enthalpies remain fairly constant, also (except for **14**α**GP** and **14**β**GP**). This behavior was reproducible in the third heating scans. Both **14**α**GP** and **14**β**GP** exhibit rather anomalous thermal behavior when compared to the shorter homologues. Besides the enthalpies of their K-D transitions being much higher than for the other homologues, the **14GP** also have some low enthalpy (presumably solid-to-solid) transitions before melting into mesophases during first heating scans; no analogous transitions were detected for any of the other **GP**. Also, the solids obtained by cooling mesophases (solid II) of **14**α**GP** and **14**β**GP** exhibit very different thermal properties from the solids obtained from solvent recrystallization (solid I).

The anomalous phase behavior of the two solid morphs of each **14GP** anomer may be a consequence of their molecular packing arrangements (*vide infra*). Another possibility, that solvent molecules are incorporated in the crystal lattices of the solvent crystallized **14GP** in solid I, is very unlikely since thermal gravimetric analyses of **14**β**GP** showed no discernible weight loss between room temperature and 130 °C (above the clearing temperature). Differences in temperatures, heats, and entropies for the D-I transitions during the first, second, and third (data not presented) heating scans of all the **GP** are negligibly small. This and other evidence indicate very little thermal decomposition even above the clearing temperatures. For both anomeric series of **GP**, T_{D-I} increases with increasing chain length and reaches a plateau near $n = 9$ that is ca. 20° higher for the β**GP**. By contrast, both the clearing temperatures and enthalpies of the D_{ho}-I transitions of cellobiose octa(*n*-alkanoates) are considerably higher for the α-anomers![10d] The entropy changes ($\Delta S = \Delta H/T_o$) were calculated for D-I transitions using the onset temperatures (T_o) from both heating (endotherm) and cooling (exotherm) peaks. The heats per mass unit for D-I transitions, also, tend to increase with increasing chain length for lower homologues and do not vary significantly when $n > 8$. This indicates that phase packing is dominated by the alkyl chains in the longer homologues. Studies on benzenehexayl hexa-*n*-alkanoates have shown that the disorder created by alkyl chains affects K-D the enthalpies and temperatures much more than those of the D-I transitions.[20] Enthalpies for the D-I transitions of the **GP** are comparable to those of benzenehexayl hexa-*n*-alkanoates[11a] and triphenylenehexayl hexa-*n*-alkanoates.[21] The higher values of ΔH and ΔS for the α anomers indicate that their mesophases are more closely packed and more ordered than those of the β anomers.

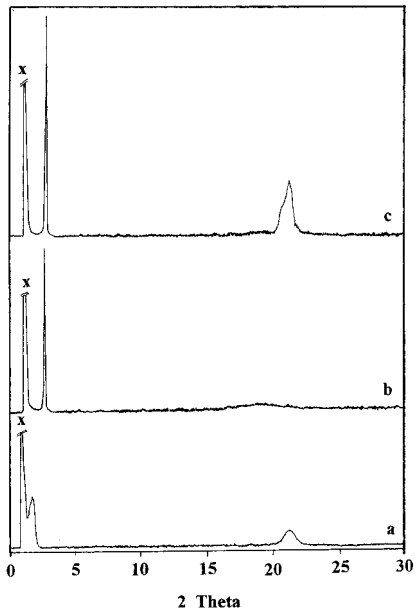

Figure 2. Powder X-ray diffractograms of solid I (a), liquid−crystalline (b), and solid II (c) phases of **14**α**GP**. × marks the scattering peak from the beam-stop cutoff.

Powder X-ray Diffraction. Diffraction data were collected on nonoriented samples of several **GP** in solid I and solid II phases at room temperature and in the liquid−crystalline phase at 52−55 °C. Figure 2 contains the diffraction patterns of **14**α**GP** as an example. The *d*-spacings in Table 2 are calculated from 2θ values using Bragg's law ($n\lambda = 2d \sin \theta$).[22]

A single, high-intensity reflection at low Bragg angles, weak, secondary reflections (with *d*-spacings in the multiples of $1/\sqrt{3}$, $1/\sqrt{4}$, $1/\sqrt{7}$, etc. of the principal low-angle reflection) in the midangle region, and a weak, broad hump at higher angles are the common features of diffractograms obtained from mesophases of all the **GP**. They indicate a hexagonal packing arrangement of columns of molecules with disordered stacking of core groups within the columns (i.e., a D_{hd} phase).[22,23] The *d*-spacing corresponding to the principal (100) reflection increases with increasing alkyl chain length (Table 2). At a

(20) Collard, D. M.; Lillya, C. P. *J. Am. Chem. Soc.* **1991**, *113*, 8577.
(21) Destrade, C.; Mondon, M. C.; Malthete, J. *J. Phys. (Les Ulis, Fr.)* **1979**, *40*, C3.
(22) (a) Glusker, J. P.; Lewis, M.; Rossi, M. *Crystal Structure Analysis for Chemists and Biologists*; VCH: New York, 1994. (b) Milburn, G. H. W. *X-Ray Crystallography*; Butterworth: London, 1973.
(23) (a) Lai, C. K.; Serrette, A. G.; Swager, T. M. *J. Am. Chem. Soc.* **1992**, *114*, 7948. (b) Baehr, C.; Frick, E. G.; Wendorff, J. H. *Liq. Crystals* **1990**, *7*, 601. (c) Sauer, T.; Wegner, G. *Mol. Cryst. Liq. Cryst.* **1988**, *162*, 97 (d) Goltner, C.; Pressner, D.; Mullen. K. *Angew. Chem., Int. Ed. Engl.* **1993**, *32*, 1660.

Table 2. 2θ (deg) and Derived *d*-Spacing (Å) Values and Miller Indices (*hkl*) of Selected **GP** in Various Phases from Powder X-ray Diffraction Measurements

	solid I[a]		liquid crystal[b]		solid II[a]	
compd	2θ	d(*hkl*)	2θ	d(*hkl*)	2θ	d(*hkl*)
14βGP	1.73	50.93 (100)	2.54	34.71 (100)	2.50	35.29 (100)
	3.04	29.03 (110)	5.05	17.47 (200)	4.97	17.75 (200)
	3.42	25.81 (200)	20.11	4.41 (001)[c]	7.53	11.74 (300)
	6.83	12.92 (400)			21.25	4.18 (001)
	21.38	4.15 (001)				
14αGP	1.77	49.87 (100)	2.68	32.91 (100)	2.78	31.74 (100)
	6.89	12.83 (400)	5.34	16.54 (200)	5.45	16.21 (200)
	21.31	4.17 (001)	19.94	4.45 (001)[c]	8.23	10.73 (300)
					21.29	4.17 (001)
8βGP	3.05	28.93 (100)	3.17	27.83 (100)	3.01	29.37 (100)
	6.07	14.55 (200)	5.55	15.90 (110)	6.03	14.63 (200)
	8.64	10.22 (210)	6.26	14.10 (200)	7.75	11.40 (210)
	18.84	4.71 (001)	8.32	10.62 (210)	19.92	4.45 (001)[c]
			19.55	4.54 (001)[c]		
8αGP		*d*	3.20	27.58 (100)		*e*
			6.48	13.62 (200)		
			19.75	4.49 (001)[c]		
7βGP	3.37	26.17 (100)	3.26	27.12 (100)	3.20	27.59 (100)
	5.98	14.78 (110)	6.54	13.49 (200)	6.41	13.77 (200)
	6.31	13.99 (200)	9.83	8.99 (300)	9.67	9.14 (300)
	20.97	4.23 (001)[c]	19.17	4.63 (001)[c]	12.37	7.15 (400)
					20.00	4.44(001)[c]
7αGP	3.24	27.28 (200)	3.34	26.39 (100)	3.03	29.09 (200)
	4.02	21.98 (110)	6.83	12.94 (200)	3.85	22.93 (110)
	6.07	14.55 (310)	10.34	8.54 (300)	5.78	15.29 (310)
	19.31	4.59 (001)	19.72	4.49 (001)[c]	19.07	4.65 (001)
6βGP	3.74	23.59 (100)	3.52	25.06 (100)	3.43	25.71 (100)
	6.57	13.45 (110)	6.00	14.72 (110)	6.83	12.94 (200)
	9.34	9.46 (210)	6.98	12.67 (200)	20.54	4.32(001)[c]
	21.14	4.19 (001)	9.95	9.66 (210)		
			20.09	4.42 (001)[c]		
6αGP	3.43	25.76 (200)	3.55	24.89 (100)		*e*
	4.14	21.30 (110)	19.17	4.62 (001)[c]		
	6.34	13.93 (310)				
	19.54	4.54 (001)				

[a] Ca. 25 °C. [b] 52−54 °C. [c] Broad. [d] Not measured. [e] Very weak peaks.

common chain length, the *d*-spacings for the α anomers are somewhat smaller than for the β anomers. The significantly smaller *d*-values of the **14αGP** may be related to the anomalously higher ΔH measured for its D-I transition. If **14αGP** is more interdigitated in its mesophase than **14βGP** and, as a result, experiences greater dispersive interactions, more energy would be required to separate the molecules into a phase with random orientations.

To probe this possibility further, intercolumnar distances (**a**) were calculated for a hexagonal lattice using the formula $\mathbf{a} = 1.154 \times d_{100}$ (where d_{100} is the *d*-spacing corresponding to the (100) reflection)[22a] and compared with molecular diameters (**2R**) calculated from MM$^+$ modeling studies[13] of energy-minimized **GP** conformations with fully extended alkyl chains (Figure 3). The calculated diameters of the α and β anomers of one chain length are essentially the same. Although **2R** is markedly greater than **a**, indicating that the **14GP** are much more interdigitated than their shorter homologues, *intra*columnar and *inter*columnar chain entanglements cannot be distinguished.

The **14GP** structures from MM$^+$ calculations predict an overall disc-like shape, although the 10 alkyl chains are projected somewhat above and below the rough plane of the core. The glucopyranose ring of the α anomer is calculated to assume a half-chair shape that places the cinnamoyl group on the anomeric carbon in an equatorial position (Figure 4a).[24] However, the

(24) This may be due to an intrinsic preference for C−O bonds, specifically, to be in equatorial positions in six-membered rings. Paquette, L. A.; Stepanian, M.; Branan, B. M.; Edmondson, S. D.; Bauer, C. B.; Rogers, R. D. *J. Am. Chem. Soc.* **1996**, *118*, 4504.

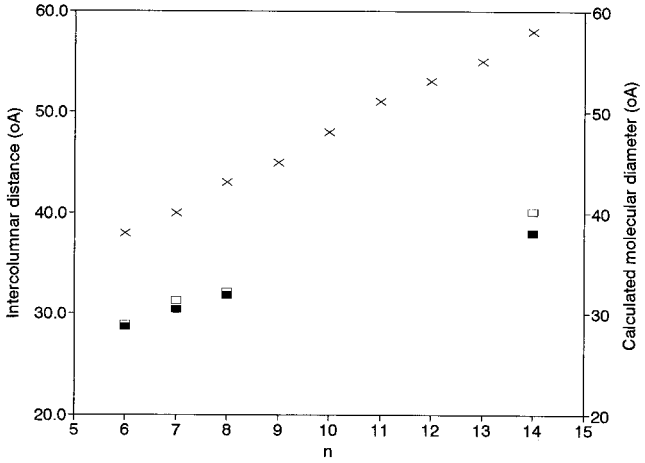

Figure 3. Intercolumnar distances from powder X-ray diffraction data of the mesophases (α series: ■; β series: □) and calculated molecular diameters (Å, from MM$^+$, X) versus alkyl chain length (*n*).

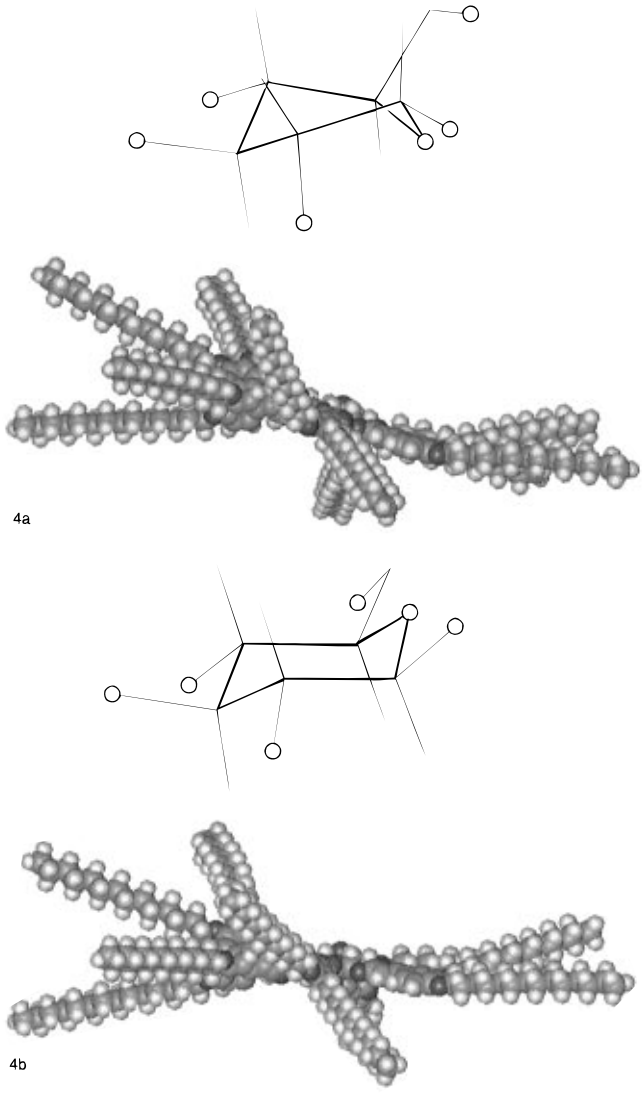

Figure 4. Energy minimized structures of **14αGP** (a) and **14βGP** (b) from MM$^+$ calculations and glucopyranose ring portions with other groups omitted for clarity; oxygen atoms are shown to indicate the ether group and where cinnamate groups are attached. The orientations of the two representations for each molecule are not correlated.

actual conformation in the neat phases may not correspond to that from the "gas phase" calculations, and the energy difference between it and a full chair conformation is probably small. *Both* the α and β anomers of **GC** are calculated to have lowest energy

full-chair conformations, requiring that the anomeric cinnamate group of the α-GC be in axial orientations. Also, X-ray diffraction studies with α-GA have led us to conclude that the anomeric alkanoyl groups of some of the homologues examined are projected axially, allowing them to occupy the space in a column near the ether group of a neighboring **GA** molecule.[8] The *β* anomer can place all of its cinnamoyl substituents in equatorial positions when the glucopyranose ring is chair-like, and that is the predicted lowest energy conformation (Figure 4b).

Solid II phases of **14*β*GP** and **14α GP** consist of hexagonally arranged molecular columns, also, with almost the same *d*-spacings as in the mesophases (Table 2). In the solid II diffractograms, the broad hump in the wide angle region of the mesophase is replaced by a narrower and more intense reflection with smaller *d*-spacing (ca. 4.2 Å), indicative of regular packing and significantly reduced motion of the core groups within a column. To be well-ordered, a **GP** column must have specific rotational orientations and specific chiral facial arrangements between neighboring molecules;[8] the broadness of the high angle peak, when compared to the sharpness of the low angle reflection, is indicative of continued orientational disorder.

Since planar, achiral disc-like mesogens typically have 6-fold (or greater) rotational symmetry and a *σ*-plane of symmetry defined by the core ring atoms, molecular orientations within a column do not usually impede crystallization from their liquid−crystalline phases. Crystallization may be suppressed by either chain entanglements, hindered rotational isomerism,[25] or other factors leading to rapid increases of viscosity at lowered temperatures that prohibit a decrease in entropy content. Conditions for crystallization of chiral molecules like **GP** that lack rotational and facial symmetry are much more severe.[8]

Diffraction patterns of the solid II phases of **6*β*GP**, **7*β*GP**, and **8*β*GP** retain the general appearance of the *d*-spacings (ca. 4.5 Å) and diffuse, weak high-angle diffraction of the mesophase, indicating a glassy phase with mesophase-like ordering of the core groups. The lack of an observable D-K transition by DSC in the initial and subsequent cooling scans and of a K-D transition in the second and third heating scans of **6*β*GP**, **7*β*GP**, and **8*β*GP**, even when samples were incubated at room temperature, is consistent with glassy phases.

Extremely weak peaks from which no meaningful information could be extracted were observed in diffractograms of solid II **6α GP** and **8α GP**. Very faint birefringent patterns were detected by optical microscopy. On these bases, the solid II phases of **6α GP** and **8α GP** appear to be amorphous glasses. Although the diffraction peaks from the solid II phases of **7α GP** were also broad and of low intensity, the two peaks in the low angle region could be indexed to an orthorhombic packing of columns.

Reflections from the solid I phases were generally broader and of lower intensity than those from the corresponding mesophases. Apparently, disorder among molecules or the distribution of their packing arrangements in a column and among columns in the (frozen) solid I phases is greater than in the (mobile) mesophases. Diffraction patterns of the solid I phases of **14α GP** and **14*β*GP** are consistent with hexagonal packing of columns. Although the *d*-spacings in the low- and mid-angle regions of the mesophase or solid II and of solid I are quite different, those from the meridional reflections remain at 4.2−4.5 Å. In fact, the solid I intercolumnar distances (**a**), 57.5 Å (α) and 58.7 Å (*β*), are ca. 20 Å longer than the **a** values for the liquid−crystalline or solid II phases and almost the same as the calculated molecular diameters (ca. 58 Å).

Calculated densities (*ρ*) of the liquid−crystalline and solid II phases of the **14GP**, using $\rho = [(\mathbf{MZ})/(\mathbf{AtN})]$ (where **M** is the molar mass, **Z** is the number of molecules present in a column slice of thickness **t**, **A** is the area of a column, and **N** is Avogadro's number), are reasonable (i.e., ca. 0.9−1.0 g/cm^3) if $\mathbf{Z} = 1$[9c,10c] when **t** is equal to the *d*-spacing. However, densities near 1 g/cm^3 for the solid I phases are calculated *only* when $\mathbf{Z} = 2$; dimeric aggregation, like that in Figure 5, is the likely cause. Similar dimeric, disk-like structures, but stabilized by hydrogen-bonding interactions, have been invoked for some tetraalkyl ether derivatives of inositols.[9c] In the absence of strong binding interactions, dimers like those in Figure 5 can dissociate easily. Such packing changes may be involved in the low enthalpy solid-to-solid transitions detected by DSC in first heating scans of **14*β*GP** and **14α GP** initially in their solid I phases.[26]

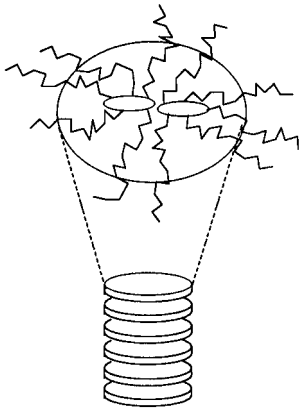

Figure 5. Cartoon representation of the proposed dimer-type aggregates of **14α GP** and **14*β*GP** in their solid I phases.

Diffractograms of solid I phases of **6*β*GP**, **7*β*GP**, and **8*β*GP** indicate hexagonal columnar packing with *d*-spacings like those of the solid II and liquid−crystalline phases. However, columns in solid I **6α GP** and **7α GP** appear to be orthorhombically packed. Except for **6*β*GP** and **7*β*GP**, the intermolecular distances within a column are >4.5 Å, indicating intracolumnar disorder.

Photo-oligomerization of GP in Various Phases and the Nature of the Oligomers. General Considerations. Samples of the α and *β* anomers of **7GP** and **14GP** have been irradiated in dilute chloroform and benzene solutions, neat discotic mesophases, solid I and solid II phases, and isotropic melt phases at ca. 320−360 nm to effect [2 + 2] photodimerizations of cinnamoyl double bonds.[18]

The absorption spectra of the **GP** in chloroform are nearly the same: for **7*β*GP**, λ_{max} 333 nm (ϵ 107 000 L mol^{-1} cm^{-1}) with a shoulder at 305 nm (ϵ 73 000 L mol^{-1} cm^{-1}) and λ_{max} 247 nm (ϵ 58 000 L mol^{-1} cm^{-1}). Thin films of neat melt and solid II phases were prepared by sandwiching the molten compounds between Pyrex discs and thermostatting them at the desired temperature. Solid I samples were irradiated as powders between Pyrex discs at room temperature. Conversions (±5%) were calculated from the loss in optical density at 333 nm (after dissolving the solid in chloroform) by assuming that [2 + 2] cycloaddition and *trans*−*cis* isomerization of cinnamoyl double bonds are the dominant photoprocesses. Previous studies demonstrate that some *trans*−*cis* isomerization occurs during even the solid state irradiations of **GC** molecules.[5c] The cyclobutane products of the [2 + 2] process do not absorb at 333 nm or at the irradiation wavelengths. Gross product structures were identified by ^{1}H NMR and IR spectroscopies, and molecular mass averages were determined by gel permeation chromatography.

(25) Kim, S.-J.; Karis, T. E. *J. Mater. Res.* **1995**, *10*, 2128.

(26) Diffraction patterns of the higher temperature crystalline phases were not recorded due to our inability to thermostat the samples with adequate precision.

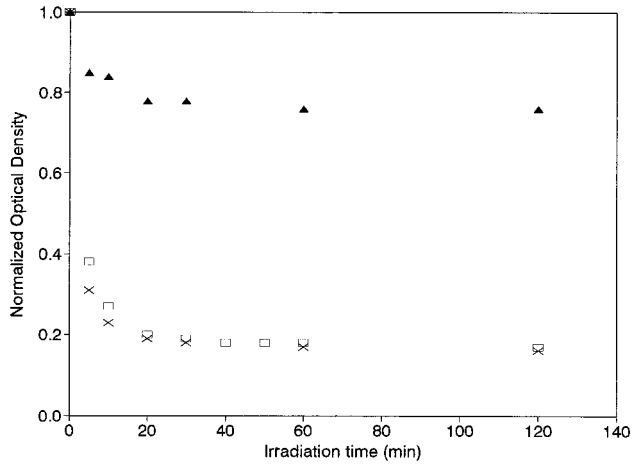

Figure 6. Change in optical density of a 10^{-5} M N_2-saturated benzene solutions of **3** (▲) at 327 nm, and **14**β**GP** (□) and **7**β**GP** (×) at 333 nm as a function of irradiation time. The OD values are normalized to time = 0.

In thicker neat samples, penetration of radiation is limited initially to regions near the surfaces; molecules farther from the surface react only after those near the surface are depleted. High conversions (ca. 90%) could be realized in relatively short times (4 h) for samples of thicknesses less than 50 μm (prepared by sandwiching an isotropic-melt between Pyrex disks).

To explore the influence of *cis* isomers on optical densities of irradiated **GP** samples,[27] a N_2-saturated benzene solution of 10^{-5} M ethyl *trans*-3,4-ditetradecyloxycinnamate (**3**, Scheme 2)[28] was irradiated to its photostationary state (pss) (Figure 6). Under these conditions, *inter*molecular cycloadditions are inconsequential since the lifetimes of the photoreactive excited singlet states[18] are in the picosecond range.[29] From integration of the olefinic protons in the ^{1}H NMR spectrum of the mixture, the *trans/cis* ratio was 3/2. Using this information and the ca. 25% reduction in optical density at 327 nm, the ϵ of *cis*-**3** at this wavelength is calculated to be 9000 L mol^{-1} cm^{-1}.

Solution Phase Irradiations. Irradiation of 10^{-5} M **7**β**GP**, **14**β**GP**, or **14**α**GP** in air-saturated chloroform or N_2-saturated benzene (under conditions where *inter*molecular cycloaddition reactions are not possible,[27] but intramolecular ones are) resulted in indistinguishable results: rapid loss of absorption at 333 nm to ca. 15% of its initial value followed by no further decreases (Figure 6). Assuming two cycloadditions per molecule of **GP** (i.e., reactions of two pairs of cinnamoyl groups), the same ϵ value for individual *cis*-chromophores of **GP** at 333 nm as that of *cis*-**3** at 327 nm and the same pss mixture of geometric isomers for the remaining **GP** double bond, the final optical density is predicted (and found) to be ca. 15% of the initial value. The absence of intermolecular reaction is supported by GPC analyses of the **GP** products (Table 3) that show a monodisperse peak corresponding to the *normalized* molecular mass (*vide infra*) of the initial species. Previously, we determined that irradiation of 1,2,3,4,6-penta-*O*-(*trans*-cinnamoyl)-(D)-glucopyranose in dilute solutions yields predominantly truxinic (head-to-head) type cyclobutanes,[5c] and a similar result is expected here.

Discotic Liquid−Crystalline Phase Irradiations. Decreases in optical density with time during irradiation of the liquid−crystalline **GP** were rapid initially and slower at later times (as in Figure 6) due to a combination of some *trans*−*cis* isomerization of cinnamate double bonds and [2 + 2] cycloadditions.[5] However, >90% decreases in optical density, corresponding to >90% conversions of double bonds to cyclobutanes, could be achieved. Apparently, some double bonds are in optimal orientations for [2 + 2] cycloaddition reactions during the early stages of irradiation. The attenuated movement of molecules caused by the initial intracolumnar−intermolecular reactions may retard cycloadditions between the remaining double bonds during the latter stages.

Table 3. Molecular Mass Averages (M_w) and Polydispersities (M_w/M_n) of Irradiated **14**α**GP** and **14**β**GP** in Various Phases

compd	% OD loss at 333 nm	irradiation period (h)	sample phase	molecular mass averages M_w	molecular mass averages M_w/M_n
14α**GP**	87[a]	2	mesophase[c]	33401	2.4
(MW = 2950)	93[b]	4	mesophase[c]	123747	2.0
14β**GP**	87[a]	2	mesophase[d]	28426	1.5
(MW = 2950)	94[b]	4	mesophase[d]	50925	1.7
	91[b]	4	solid II[e]	58994	2.1
	82[b]	4	solid I[e]	31419	3.8
	92[b]	2	melt[f]	18707	1.3
	83[a]	2	solution[g]	3662	1.0
	0[a]	0		3721	1.0
	0[b]	0		3870	1.0

[a] Data from GPC instrument 1. [b] Data from GPC instrument 2. [c] At 95 °C. [d] At 110 °C. [e] At 25−35 °C. [f] At 130 °C. [g] 10^{-5} M in N_2-saturated benzene at ca. 30 °C.

In spite of the large conversions, *the optical textures of the liquid−crystalline phases of* **7**α**GP**, **7**β**GP**,[30] ***14***α**GP**, *and* **14**β**GP** *were not visibly changed by extended irradiation*. They are unaffected by cooling to room temperature, where the monomers are solids or by heating to where the monomers are isotropic liquids. This observation and knowledge of the initial packing arrangement of the monomers requires that the oligomer chains be unbranched.

For example, the optical texture of the material obtained after irradiation of **14**β**GP** in its mesophase at 110 °C to ca. 85% reduction in optical density faded gradually and disappeared only near 230 °C; it did not reappear upon cooling. The optical texture was also lost when oligomerized **14**β**GP** was dissolved in chloroform and reprecipitated. Another sample of oligomerized **14**β**GP** was cooled to room temperature, and its DSC thermograms were recorded; no transitions were detected upon initial heating to 250 °C or upon cooling the heated sample to room temperature. Similarly, after a sample of **7**α**GP** (T_{D-I} 81 °C), had been irradiated in its liquid−crystalline phase at 65 °C to ca. 80% conversion, its optical clearing temperature was near 260−280 °C and birefringence did not reappear upon cooling.

Another sample of **14**β**GP** that had been irradiated at 110 °C (to ca. 85% conversion) was cooled to room temperature, and its X-ray diffraction pattern was recorded (see supporting information). As expected, an intense low-angle peak and a diffuse high-angle peak like those of the unirradiated liquid−crystalline phase were present. The *d*-spacing of the (100) reflection, 35.6 Å, is 0.9 Å larger than in the unirradiated liquid−crystalline phase. The small increase may be due to an ancillary consequence of bringing the facial portions of linked **GP** cores closer together. Unfortunately, the high angle peak was too weak to determine with reasonable precision the magnitude of the decrease in interfacial distances. When the oligomerized sample was heated above its melting temperature and then recooled, the lower angle peak lost most of its intensity and became broader, as expected from the optical microscopic observations.

Infrared spectra of **14**β**GP** samples irradiated at 110 °C showed the appearance of a saturated ester carbonyl stretch (1745 cm^{-1}) and disappearance of bands from the unsaturated ester (1720 cm^{-1}) and double bond (1630 cm^{-1}) (see supporting information). ^{1}H NMR spectra of irradiated samples lacked

(27) Lewis, F. D.; Oxman, J. D.; Gibson, L. L.; Hampsch, H. L.; Quillen, S. L. *J. Am. Chem. Soc.* **1986**, *108*, 3005.

most of the olefinic proton resonances of the **GP** and included new aliphatic proton resonances around 3−4 ppm from cyclobutane protons. The severe broadening of proton resonances from groups near the molecular core (cyclobutyl moieties, aromatic rings, and -OCH_2- groups of the alkoxy chains) indicate very long relaxation times (and impeded torsional motions) due to the formation of large oligomers. Although ^{1}H NMR spectra of the monomeric products from solution irradiation show more resolved and narrower resonances for cyclobutyl and other protons near the core, some of the aromatic protons are also broadened (see supporting information). Mobility of the alkyl chain protons is not expected to be affected by the [2 + 2] cycloaddition reactions and their resonances remain narrow for the irradiated samples.

From molecular mass averages (M_w) determined by gel permeation chromatography (Table 3), 5−8 monomers[31] were linked during irradiation of liquid−crystalline **14**β**GP** to ca. 85% conversion. At >90% conversion (by increasing the irradiation time), oligomers whose molecular mass averages correspond to 8−14 **GP** units (Table 3) are formed. Curiously, irradiation of **14**α**GP** in its D_{hd} liquid−crystalline phase at 95 °C produced oligomers of much higher average molecular masses, corresponding to the linking of 16 to 33 monomers at similar photoconversions. The polydispersities of these oligomers, near 2, are surprisingly low considering the nature of the linking process.

As mentioned, MM^+ based computations indicate that a half-chair conformation for the glucopyranose rings of the α**GP** is lowest in energy, and there is precedent for axial projections of less bulky anomeric groups in related discotic phases.[8] Although the much larger size of the dialkoxycinnamoyl groups of α**GP** makes a packing arrangement like that stabilizing the full-chair conformations of αGA molecules less likely, *axial* projection of the anomeric groups of the α**GP** would promote intermolecular cycloadditions, and we consider this a possible explanation for the greater degree of oligomerization in the α series.

Solution CD spectra of **14**β**GP** and the oligomers obtained from its irradiation (>80% conversion) in the liquid−crystalline phase display very little dichroism (ca. 1 mdeg for either sample at 0.08 mg/mL concentrations) where the corresponding absorption spectra have high optical densities. Several glucopyranose and other saccharide derivatives containing *p*-methoxycinnamoyl chromophores are known to have very high dichroic absorptions with exciton-coupled bands, and intensity of the dichroism increases in an additive fashion as the number of chromophores on the saccharide core is increased.[32] The **GP** molecules and their oligomers may favor a conformation that essentially cancels the dichroic absorption of individual cinnamoyl chromophores rather than leading to their additivity.[33]

Solid II Phase Irradiations. Irradiation of **14**β**GP** in its solid II phase (obtained by cooling the liquid−crystalline phase) at 25−35 °C and mesophase at 110 °C under otherwise comparable conditions led to similar conversions. Initial optical textures of the solid II samples were maintained after irradiation as well, but heating and cooling did not convert them to a texture like that in Figure 1c: the texture of a sample irradiated to >90% conversion was intact up to ca. 220 °C and became completely isotropic only at ca. 250 °C; like samples oligomerized in their liquid−crystalline phases, the solid II oligomer lost its birefringence permanently once heated above its clearing temperature was increasingly deformable by pressure as the temperature was increased. Completely analogous results were obtained upon irradiation of **7**α**GP** and **7**β**GP** in their solid II phases.[30] Even at elevated temperatures, the molecular motions necessary to form a liquid−crystalline phase are blocked by the covalent linkages between **GP** moieties.

Although powder diffraction patterns indicate almost identical hexagonal columnar packing for the liquid−crystalline and solid II phases (Table 2), their comparable reaction rates are surprising since the more rigid solid should be more demanding topochemically than the mesophase.[18] Either a large fraction of the cinnamates must be frozen at near bonding distances and orientations, or significant motion must be possible.

Molecular mass averages of oligomers from the solid II phase of **14**β**GP** irradiated for 4 h at 25−35 °C (>90% conversion) correspond to 7−15 linked **GP** units, slightly more than in the mesophase (Table 3). On the basis of the optical micrographs, the oligomers must be cylindrical in shape and packed in parallel columns (like the monomeric phase) as formed. However, it and the other solid II oligomers cannot be converted by heating to liquid−crystalline phases.

These observations indicate that cylindrical oligomers formed initially from the columnar phases of **GP** are neither rigid nor in their preferred conformations. Preassembly of the columns forces the oligomers to be columnar. When provided with the opportunity to explore other shapes, the cylinders "unwind". In order for such shape changes to occur, at least some of the **GP** units in each cylinder must be linked through no more than one [2 + 2] cycloaddition (Scheme 3a); if two (or more) cyclobutane rings are shared by a pair of **GP** units, escape from a face-on orientation is essentially blocked (Scheme 3b).

Solid I Phase Irradiations. Irradiation of **14**β**GP** in its solid I phase (obtained by recrystallization from solvent) at 25−35 °C was slower than in its liquid−crystalline or solid II phase; 4 h were needed for ca. 80% conversion. GPC analysis revealed a low degree of oligomerization with higher polydispersity (Table 3). A large sharp peak with elution time corresponding to the monomer and a smaller one that may be from dimers, along with broad and less prominent peaks for oligomers (Figure 7) are present. Clearly, *intra*molecular [2 + 2] processes are more favored in the solid I phase than in the solid II and liquid−crystalline phases. Additionally, the molecular pairing nature of the solid I columns of the **14GP** (Figure 5) suggests that the oligomers derived from them are branched.

Irradiation in the Melt Phases. Among the neat phases of **14**β**GP**, the "isotropic" melt phase at 130 °C underwent the fastest conversion (ca. 90% in 2 h) to photoproducts. However, GPC analysis of this sample showed that only 4−5 monomers

(28) Except for a small blue shift of the lowest energy band and an expected 5-fold reduction in ϵ, the absorption spectrum of **3** in chloroform or benzene is like those of the **GP**: λ_{max} 327 nm; ϵ 20 300 L mol^{-1} cm^{-1}.

(29) Lewis, F. D.; Quillen, S. L.; Elbert, J. E. *J. Photochem. Photobiol., Part A* **1989**, *47*, 173.

(30) The **7**α**GP** and **7**β**GP** exhibit photochemical behavior that is similar to their tetradecyl homologues. Irradiations of mesophases near the clearing temperatures or of solid II phases at 25−35 °C gave high photoconversions with no detectable changes in optical textures. Proton NMR and IR spectra of the photoproducts were comparable to those of similarly irradiated tetradecyl homologues. However, GPC analyses of oligomers from irradiation of the various phases of the **7GP** led only to very small peaks from which no usable information could be extracted. The oligomers were not completely soluble in the initial eluent, THF, and do not have sufficiently different indices of refraction from a second eluent, toluene, to allow reasonable signals from the RI detector. For that reason, we have emphasized data from the longer homologues.

(31) Since the two GPC instruments employed gave slightly different M_w values for unirradiated **14**β**GP**, the degrees of oligomerization have been calculated assuming the monomeric molecular masses from the appropriate data set (rather than using 2950, the correct molar mass).

(32) Nakanishi, K.; Berova, N. In *Circular Dichroism*; Nakanishi, K., Berova, N., Woody, R. W., Eds.; VCH: New York, 1994; pp 361−398, and references cited therein.

(33) (a) Zhao, N.; Lo, L.-C.; Berova, N.; Nakanishi, K.; Tymiak, A. A.; Ludens, J. H.; Haupert, G. T., Jr. *Biochemistry* **1995**, *34*, 9893. (b) Wiesler, W. T.; Berova, N.; Ojika, M.; Meyers, H. V.; Chang, M.; Zhou, P.; Lo, L.-C.; Niwa, M.; Takeda, R.; Nakanishi, K. *Helv. Chim. Acta* **1990**, *73*, 509.

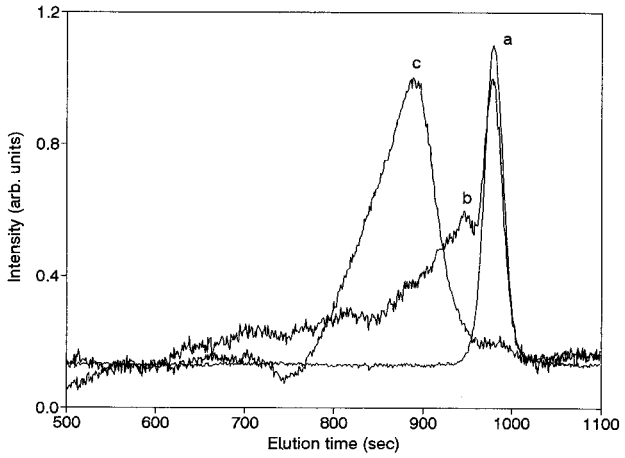

Figure 7. Gel permeation chromatograms for **14**β**GP** (a) before and (b) after 4 h irradiation in the solid I phase at 25−35 °C, and (c) after 2 h irradiation in the melt ("isotropic") phase at 130 °C. The shape of the peak for the **14**β**GP** product after irradiation of a 10^{-5} M N_2-saturated benzene solution is virtually the same as in (a).

Scheme 3

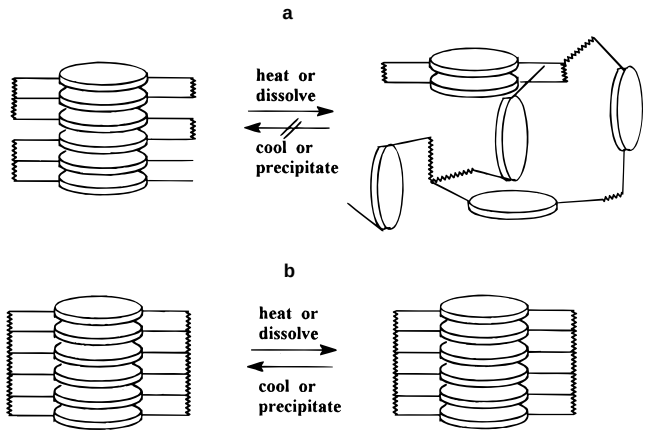

were covalently linked (Table 3 and Figure 7c). When cooled, the irradiated sample was glassy, and its optical texture lacked any discernible birefringence. The disorganization of the melt phase makes the topology for *inter*molecular reaction more difficult to attain. Also, the photoproducts are unable to pack in columns when cooled.

The mode of intermolecular reaction in the melt phase should be very different from that in the solid and liquid−crystalline phases. Individual molecules in the melt are much more mobile in all dimensions and lack orientational and positional order. Most importantly, one **GP** may be linked to as many as *five* other **GP** molecules; highly branched oligomers are possible.[5a] In all of the columnar phases except those from solid I of the **14GP**, each **GP** can be linked to no more than two other **GP** molecules by virtue of packing constraints. The observation of low-molecular mass oligomers (ca. four linked monomers) from irradiation of **14**β**GP** in its melt phase indicates that the proximity among the five cinnamate groups on each **GP** leads to preferred *intra*molecular reactions and that columnar order among **GP** molecules is a key entropic factor for effective [2 + 2] *inter*molecular cycloadditions.

The behavior of melt phase **14**β**GP** is in sharp contrast to irradiation results from isotropic hexakis-*N*-(4-tetradecyloxycinnamoyl)hexacyclen from which very high molecular weight, highly-branched polymers were obtained.[5a] In that case, *inter*molecular reactivity is clearly favored over the *intra*molecular since cinnamoyl groups are kept farther apart in a hexacyclen molecule than in a **GP**.

Conclusions

The **n**α**GP** and **n**β**GP** ($n = 6-8$, 10, and 14) investigated here form enantiotropic discotic columnar liquid−crystalline phases that persist over wide temperature ranges; clearing temperatures are intrinsically higher in the β anomeric series. They increase with increasing chain lengths and plateau at $n \geq 10$. Columnar packing has been identified in some of the solid phases, also. Columns are arranged hexagonally or orthorhombically.

Irradiation of dilute solutions of **GP** homologues leads only to *intra*molecular [2 + 2] dimerizations of no more than four cinnamoyl double bonds per molecule. Although short (4−5 **GP** units), probably branched oligomers are produced by irradiation of the neat melt (nonbirefringent) phases, reaction continues to be primarily *intra*molecular. The oligomers are nonbirefringent and glassy when cooled; more than four double bonds per molecule can be induced to react.

After photoinduced oligomerization, the columnar arrangements of **GP** molecules in their neat discotic liquid−crystalline and solid II phases are retained to temperatures ca. 100° above the monomer clearing transitions. Under these conditions, reaction is exclusively *intra*columnar, primarily *inter*molecular, and (except for the solid I phase of **14GP**, where two molecules are along a columnar cross-section) unbranched. In the most favorable cases, more than 30 monomer units of **GP** have been linked in unbranched chains while retaining, for the first time, the columnar organization of the monomers. The oligomers, as produced initially from these phases, are nanoscale cylinders of one diameter and varying lengths. Once the initial oligomer conformation is lost (via heating to much higher temperatures than the monomer clearing points or via dissolution), it is not reestablished (upon cooling or precipitation) due to the occurrence of some [2 + 2] cycloadditions that lead consequently to increased potential mobility within the polymer chains.

Results from these studies pose a challenge for construction of cylindrical oligomers that are shape-persistent at high temperatures and in solutions.

Acknowledgment. We are indebted to Mr. Ashabir Fiseha and Dr. Steven Pollack of the Chemistry Department, Howard University, and Dr. Tai Ho of the Naval Research Laboratory, Washington, DC, for use of their gel permeation chromatographs. Financial support to RGW by the National Science Foundation (Grants CHE-9213622 and CHE-9422560) is gratefully acknowledged. In memory of Professor Ernesto Giesbrecht, an excellent scientist, a wonderful person, and a visionary whose pioneering efforts helped make the Instituto de Quimica of the Universidade de Sao Paulo a premiere scientific institution.

Supporting Information Available: One table of solvents for recrystallizations and silica gel chromatographic purifications, seven figures (DSC thermograms of **8**β**GP**, **14**α**GP**, and **14**β**GP**, powder X-ray diffractograms of **14**β**GP** in various phases, infrared and ^{1}H NMR spectra of **14**β**GP** before and after irradiation of a neat, thin, liquid−crystalline film, and gel permeation chromatograms before and after irradiation of **14**β**GP** in various phases), and ten ^{1}H NMR and ten FT-IR spectra of the **GP** (30 pages). See any current masthead page for ordering and Internet access instructions.

JA961665X